Direct Current Degradation and Electrophysical Properties of ZnO-Polyaniline Composites

M. Ghafouri a,* , M. Ahdi b and B. Tavakkoli a

Received: 02.12.2024 & Accepted: 03.06.2025

Doi: 10.12693/APhysPolA.147.475

*e-mail: ghafouri1355@iau.ac.ir

This study investigates the electrical nonlinear properties of ZnO-polyaniline composite varistors before and after direct current degradation, as well as the influence of ZnO content variation in the composite. All samples were fabricated via the hot-pressing method at a temperature of 130°C and a pressure of 60 MPa. The results show that increasing the ZnO content reduces both the nonlinear coefficient (from 8.3 to 7.7) and the breakdown voltage (from 560 to 340 V). However, direct current degradation induced a notable rise in the nonlinear coefficient, most prominently in the 80% ZnO sample, where it increased from 8.3 to 11.1. All samples showed a slight increase in breakdown voltage ($\sim 40 \text{ V}$) alongside a reduction in leakage current. Microstructural analysis via scanning electron microscope reveals two distinct phases, i.e., ZnO grains and polymer-rich intergranular regions. Post-degradation scanning electron microscope analysis indicated no significant changes in ZnO grain morphology, suggesting that the observed electrical shifts are primarily linked to interfacial modifications.

topics: composite varistor, direct current degradation, electrical characterization, breakdown voltage

1. Introduction

Zinc oxide (ZnO)-based varistors with high non-linear coefficients are highly effective as surge protectors. They operate by transitioning to a highly conductive state above their breakdown voltage, thereby suppressing voltage surges. The non-ohmic behavior of ZnO varistors arises from thermionic emission at low electric fields and several conduction mechanisms at high fields [1, 2]. This behavior is intrinsically related to their microstructure, which consists of three distinct phases: (i) the Birich phase surrounding ZnO grains, (ii) the spinel phase at grain boundaries, and (iii) the ZnO grains themselves [3–5].

In ZnO-based varistors, the grains and their adjacent insulating intergranular layers form double Schottky barriers at the grain boundaries. These potential barriers play a crucial role in regulating charge carrier conduction under varying electric field conditions [6–9]. However, varistors with simpler microstructures exhibit superior energy absorption due to their extensive effective grain boundary regions [10]. These extended boundaries enhance energy dissipation during voltage surges, improving overvoltage protection capabilities [10].

Bismuth oxide is the most important ingredient to produce nonlinear behavior in ZnO-based varistors, but its high volatility, reactivity, low melting point, and tendency to form complex microstructures have prompted researchers to investigate alternative materials [11, 12]. Among the explored substitutes, Zn–Pr-based and polymer-based varistors have shown particular promise due to their advantageous properties [13–19]. Polymer incorporation improves both the homogeneity and density of active barriers in the varistor structure, thereby enhancing performance. Moreover, eliminating metal oxide additives can further reduce the breakdown voltage, improving energy absorption and surge protection capabilities [16–20].

The performance of a varistor depends not only on its primary materials but also on various additives that significantly influence its functionality. A critical aspect affecting the performance of a varistor is degradation, which occurs through multiple mechanisms [21–25]. Two particularly important degradation mechanisms have been identified in the literature:

- (i) Under an applied electric field, zinc ions migrate to the depletion layer due to chemical interactions between ZnO grains and grain boundaries. This process increases the leakage current while decreasing the potential barrier height. Notably, greater degradation correlates with higher leakage currents [26, 27].
- (ii) Oxygen desorption occurs during degradation, despite prior chemical absorption at the grain boundaries [21, 26].

^aDepartment of Physics, Shabestar Branch, Islamic Azad University, 5381637181, Shabestar, Iran

^bFaculty of Physics, University of Tabriz, 5166616471, Tabriz, Iran

Reducing leakage current is one way to mitigate its impact. However, various other factors, such as heat, ultraviolet (UV) light, mechanical stress, and humidity, can also lead to polymer degradation. Degradation can cause polymers to become brittle, fade, or crack [28–31].

In addition to these phenomena, Joule heating represents a particularly significant degradation mechanism in composite varistors. This effect stems from their relatively higher leakage current compared to ceramic varistors, promoting oxygen loss and operational damage. While reducing leakage current can mitigate this impact, other environmental factors — including heat, UV radiation, mechanical stress, and humidity — may also induce polymer degradation [28–31]. Such degradation can manifest as brittleness, discoloration, or cracking of the polymer matrix. Furthermore, the interaction between ceramic fillers and the polymer matrix may accelerate degradation, with thermal energy and Joule heating potentially exacerbating these effects [32]. Although numerous studies have examined degradation mechanisms in ZnO-based ceramic varistors, the degradation behavior of polymerbased varistors remains unexplored in the literature. This study investigates the current-voltage (I-V)characteristics of ZnO-polymer composite varistors both before and after direct current (DC) degradation.

2. Experimental details

The doped polyaniline (PANI) used in this study was synthesized from aniline monomer in its emeraldine base form (purchased from Merck) following the procedure described in [33]. PANI functions as a critical secondary phase in the composite varistors, playing a significant role in establishing their nonlinear electrical properties. This additive enhances the varistor's electrical properties, enabling improved performance across varying voltage conditions while facilitating the formation of barrier structures at grain boundaries. These barrier structures are essential for establishing the non-ohmic behavior characteristic of these devices. Since composite varistors require an intergranular phase with low conductivity ($\sigma \approx 10^{-10} \text{ S/cm}$), the PANI was de-doped for 8 h using a 2 M ammonia solution [33]. The resulting product was dried at 70°C for 96 h and underwent multiple grinding cycles. To further enhance grain boundary resistivity, high-density polyethylene (HDPE) powder (additive-free, Tabriz Petrochemical Company) was incorporated as a secondary polymer. This HDPE addition not only improves electrical properties but also enhances the composite's mechanical stability [34–37]. ZnO powder (99.9% purity, Merck) was used as the primary component for producing ZnO-polymer composite varistors. All powdered materials were sieved through a 200 mesh U.S. standard sieve (particle size $< 70~\mu m$). Due to the polydisperse nature of polymers, all constituents were mixed according to their mass ratios. To optimize composite varistor performance, samples were prepared with the following compositions by mass:

- 80% ZnO + 20% polymer matrix,
- \bullet 85% ZnO + 15% polymer matrix,
- 90% ZnO + 10% polymer matrix.

The polymer matrix itself consisted of a 3:1 mass ratio of PANI to HDPE. All components were precisely weighed (10^{-4} g accuracy) before processing to ensure compositional accuracy.

All samples were prepared under identical processing conditions. The powder mixtures were homogenized in a ball mill for 4 h to ensure compositional uniformity. The resulting composites were then formed into disk-shaped varistors (diameter 10 mm, thickness 250 μ m) via hot pressing at 130°C under a pressure of 60 MPa.

To investigate the I-V characteristics, a twoprobe method was employed, using a 10 mm copper probe as the lower electrode and a 6 mm copper probe as the upper electrode. The I-V characteristics of the samples were re-examined after exposure to DC stress. All samples were subjected to voltages above their respective threshold values. The resulting changes in electrical properties were assessed. Microstructural analysis was performed using a MIRA3 TESCAN scanning electron microscope (SEM).

3. Results and discussions

3.1. The I-V characteristics and nonlinearity

The current–voltage (I-V) characteristic represents the most critical property of varistors. Figure 1 demonstrates the nonlinear behavior of all samples measured at room temperature, revealing a consistent decrease in breakdown voltage with increasing ZnO content. The corresponding quantitative data are presented in Table I.

All samples exhibited leakage currents in the microampere range, increasing to over 6 mA in the breakdown region. Samples containing less than 80 wt% ZnO showed significantly higher breakdown voltages, while compositions exceeding 90 wt% ZnO displayed near-ohmic characteristics. Consequently, these prepared samples proved unsuitable for practical applications.

Before discussing the results presented in Table I, it is essential to explore the underlying causes of the observed nonlinear behavior in the system. The observed nonlinear behavior originates from the varistor's microstructure, comprising conductive ZnO grains and insulating intergranular phases (PANI/HDPE). This configuration creates potential barriers (Schottky barriers) between grains,

TABLE I Comparative analysis of sample performance before degradation (B. Deg) and after degradation (A. Deg).

| Sample | Nonlinear coef. | | Breakdown voltage [V] | | Potential barrier [eV] | |
|------------|-----------------|---------|-----------------------|---------|------------------------|---------|
| | B. Deg. | A. Deg. | B. Deg. | A. Deg. | B. Deg. | A. Deg. |
| (80% ZnO) | 8.34 | 11.1 | 560 | 600 | 0.0555 | 0.0607 |
| (85% ZnO) | 7.33 | 8.3 | 400 | 440 | 0.0615 | 0.0722 |
| (90% ZnO) | 7 71 | 8.08 | 340 | 380 | 0.0788 | 0.0874 |

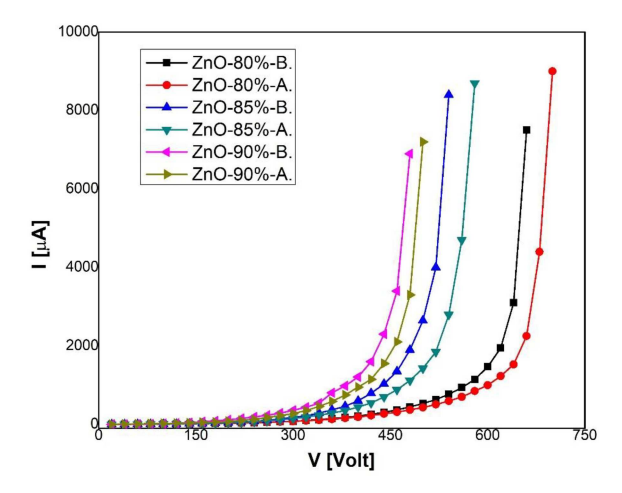


Fig. 1. The I-V characteristic of the samples before (B.) and after (A.) degradation.

where narrow intergranular regions form back-to-back Zener diodes that trap and block charge carriers [38–40]. Under an applied electric field, charge carrier tunneling through these barriers produces a nonlinear response (as will be discussed in detail later).

Table I presents the correlation between ZnO content and nonlinear properties. Increasing the ZnO content in the mixture reduces the nonlinear coefficient from 8.3 to 7.7, which is accompanied by a corresponding decrease in breakdown voltage from 560 to 340 V. This characteristic of varistor behavior stems directly from its microstructural features. A varistor consists of multiple micro-varistor elements, each defined by the grain-intergranulargrain structure. The total breakdown voltage depends on the number of active micro-varistors between the electrodes, which is described by $V_b = (V_r d)/e$, where V_b is the breakdown voltage per barrier (micro-varistor), V_r is the breakdown voltage of the device, d is the average grain size, and e is the sample thickness [20]. In composite varistors, the breakdown voltage of individual microvaristors depends on two key factors, i.e., the space between grains and the presence of polymer additives (PANI/HDPE) that modify the charge tunneling behavior [41].

Charge carrier tunneling will not initiate at a given voltage until the distance between two grains reaches a specific threshold. This condition can be

met by increasing the ZnO content in the composite, which reduces the spacing between conductive grains. At a constant thickness, increasing the ZnO content effectively reduces the space between grains, thereby lowering both the breakdown voltage and the potential barrier height. However, higher ZnO content simultaneously increases electron trap sites at the grain boundaries, resulting in elevated leakage currents.

The increased leakage current reduces the nonlinear coefficient according to

$$I = KV^{\alpha} \rightarrow \alpha = \frac{\ln(I_2) - \ln(I_1)}{\ln(V_2) - \ln(V_1)},$$
 (1)

where V is applied voltage, K is a constant, I is the passing current through the sample between two electrodes, and α is the nonlinear coefficient determined by the slope of the curve $\ln(I)-\ln(V)$.

Figure 2 presents SEM micrographs corroborating the structural evolution with ZnO content. At low ZnO concentrations (Fig. 2a), the polymer matrix forms a continuous phase. With increasing ZnO content (Fig. 2c), the polymer phase diminishes, leaving voids between ZnO particles. To validate this assertion, analysis via ImageJ software was used to calculate the particle-to-void ratio for each composition (Fig. 2d–f corresponds to Fig. 2a–c, respectively).

3.2. Degradation and nonlinearity

All samples were subjected to voltages above their respective threshold values (voltage equivalent to the ~ 1 mA electric current). Details are shown in Fig. 3.

The I-V characteristics of the samples were measured at room temperature after applying DC degradation, using the same samples that were previously tested for their initial I-V behavior (Fig. 1). As shown in Fig. 1 all samples display a similar response after the application of electric current. Notably, the breakdown voltage increased by ≈ 40 V. However, the key observation is that the leakage current decreased while the nonlinear coefficient showed an increase (Table I). The observed decrease in leakage current and increase in breakdown voltage likely result from component redistribution within the HDPE matrix induced by Joule heating.

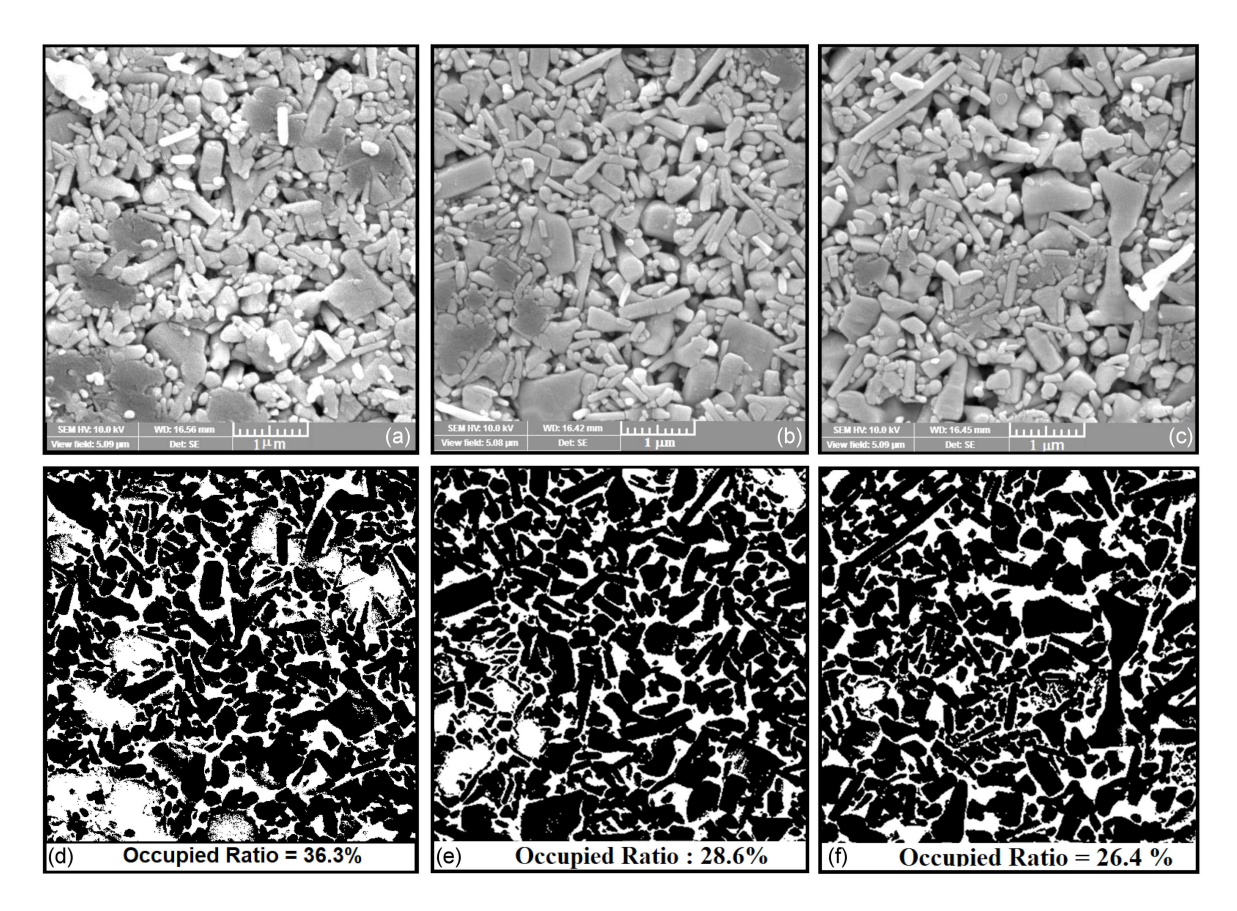


Fig. 2. SEM micrographs of samples before degradation: (a) 80% of ZnO, (b) 85% of ZnO, (c) 90% of ZnO, and (d-f) their related occupied ration.

This particle redistribution, known as phase separation, is a well-documented phenomenon in polymer composites [42]. Joule heating arises from the flow of electric current, as described by the equation $Q = R I^2 t$, where Q is generated heat energy, R is resistance, I is electric current, and t is time. Although the electric current is relatively low (~ 9 mA), it induces a rise in the functional temperature. When the temperature approaches 50°C, thermal runaway occurs, leading to a further temperature increase beyond 70°C (Fig. 3). Following degradation, thermal stress becomes evident as the physical structure of the samples undergoes noticeable changes. In particular, the edges of the samples located outside the contact area appear crumpled.

The SEM imaging was also performed on degraded samples. While DC degradation induced measurable changes in electrical properties (see Fig. 1 and Table I), post-degradation SEM analysis revealed no significant alteration to the ZnO grain morphology or bulk polymer phase distribution (see Fig. 4). This confirms that the observed increases in nonlinearity and barrier heights stem primarily from interfacial modifications (e.g., PANI redistribution or trap-state passivation) rather than bulk microstructural reorganization. Similar behavior has been reported in polymer-composite varistors [16–19]. In contrast to ceramic varistors [7, 21],

where grain-boundary phases evolve under stress, in composite systems, degradation is governed by the polymer matrix's nanoscale response to Joule heating.

As discussed earlier, the nonlinear behavior originates from the formation of a Schottky barrier at the grain—intergranular boundary. To confirm this effect, Pianaro et al. [40] proposed a model describing the relationship between current density and electric field as follows

$$J = AT^2 \exp\left(\frac{\beta E^{1/2} - \varphi_B}{k_{\rm B}T}\right). \tag{2}$$

Here, A denotes the Richardson constant, β is a parameter related to the width of the potential barrier, φ_B represents the interface potential barrier height, while T and $k_{\rm B}$ represent the temperature and Boltzmann constant, respectively. According to this model, as the electric field increases, the barrier height decreases, facilitating enhanced charge carrier tunneling. At a fixed temperature, the Schottky barrier height (φ_B) can be determined directly by measuring the current density in the ohmic region. This is achieved by plotting the $\ln(J)-E^{1/2}$ or, equivalently, $\ln(I)-V^{1/2}$ dependence. The potential barrier height is determined by the intercept of this curve (Fig. 5). The calculated values are summarized in Table I. The results indicate that increasing

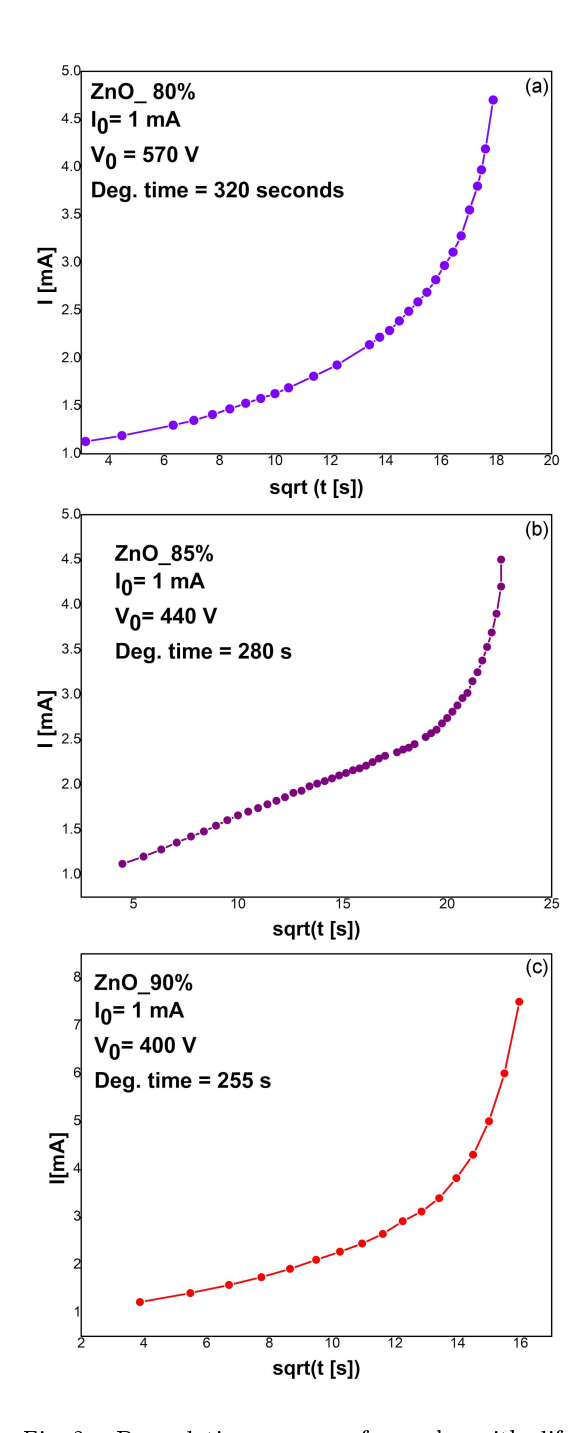


Fig. 3. Degradation process of samples with different compositions (a-c).

the ZnO content in the mixture raises the potential barrier height. However, this trend contrasts with the observed reduction in breakdown voltage and differs from the behavior reported for Si-PANI-PE (where PE stands for polyethylene) composite varistors [36]. This phenomenon may arise from the complex interplay between microstructural characteristics and electrical properties in these materials. Although increased ZnO content enhances the potential barrier height, it simultaneously modifies the overall conductivity and tunneling behavior of charge carriers.

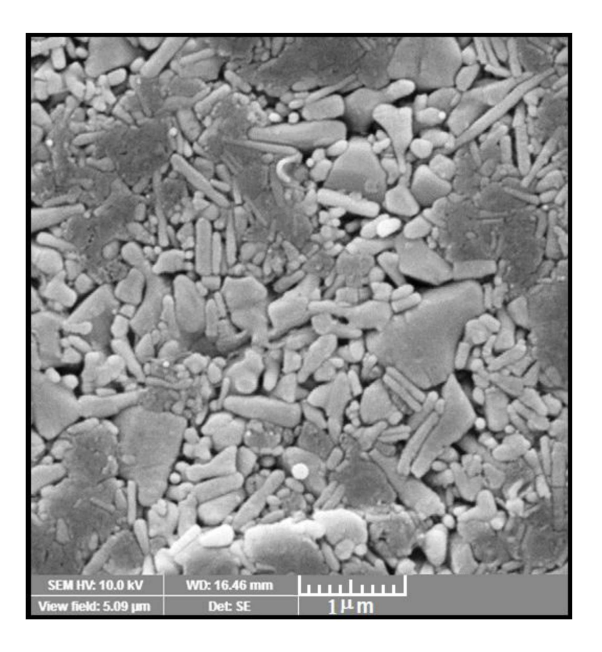


Fig. 4. Post-degradation SEM micrographs for the sample with 80% ZnO content. No microstructural changes were observed post-degradation.

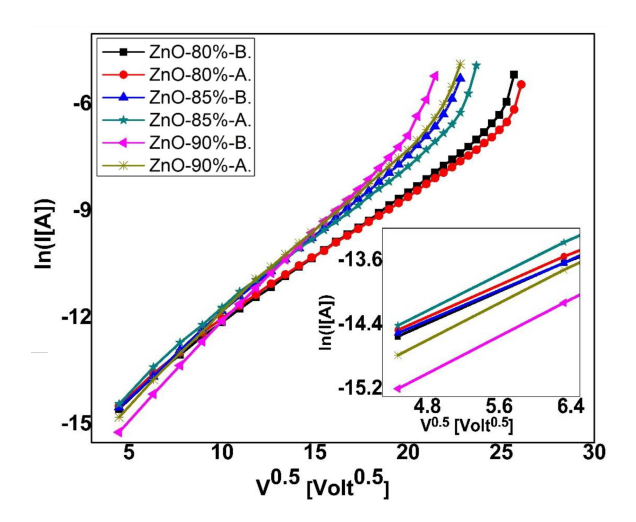


Fig. 5. The obtained dependence $\ln(I)-V^{1/2}$ for calculating the potential barrier of the samples.

To clarify this contradiction in more detail, it is necessary to revisit and explain some fundamental quantities.

- The breakdown voltage of a varistor is primarily determined by the number of grain boundaries present between the electrodes.
- The potential barrier height at the grain boundaries plays a critical role in determining the electrical characteristics of a varistor.

Typically, the increase in a potential barrier height is associated with a higher breakdown voltage. However, the introduction of PANI disrupts this established relationship. Acting as a dopant, PANI significantly modifies the electrical properties in the

pre-breakdown regime through three primary mechanisms: (i) the reduction of the Schottky barrier height, (ii) the alteration of intergranular resistivity, and (iii) the modulation of charge transport in the high-current region.

Consequently, the incorporation of PANI can invert the conventional barrier height—breakdown voltage correlation. This phenomenon can be attributed to the inherent properties of organic polymers, which typically either exhibit a complete absence of intrinsic charge carriers or contain them in limited amounts. For conjugated polymers, including PANI, charge carriers are typically introduced through a partial oxidation or reduction process involving electron acceptors or donors, respectively. This doping mechanism facilitates the incorporation of charge carriers into the polymer structure, enabling it to influence the electrical properties of the composites, which increases its conductivity [43].

Environmental factors such as diffusion of doping elements and oxygen can gradually degrade the potential barriers, resulting in alterations to the varistor's electrical characteristics over time. In contrast, the breakdown mechanism itself, typically initiated by a tunneling process and accompanied by hole generation, can cause a sudden reduction in the barrier height and a sharp increase in current. This occurs despite the fact that the breakdown voltage per barrier remains independent of the material's composition or processing [8]. Therefore, although a higher potential barrier height is often correlated with a higher breakdown voltage, there can be complex interactions among grain structure and doping profile. Besides, the breakdown mechanisms can lead to deviations from this expected behavior [44, 45].

Another important issue regarding the $\ln(I) - \sqrt{V}$ dependence in Fig. 5 is that it deviates from the ideal linear behavior expected for pure "Schottky emission" due to several factors related to the complex microstructure and conduction mechanisms in ZnO–PANI composites. This is due to the fact that these composites consist of ZnO grains (conductive) and polymer-rich intergranular regions (insulating), creating a heterogeneous system. Although Schottky emission (thermionic emission over barriers) dominates at low fields, other mechanisms contribute as the voltage increases, which causes a deviation from the linear response. The important parameters are as follows:

- Poole—Frenkel emission or field-assisted thermal excitation of trapped charges in the polymer matrix [43]. PANI's emeraldine base contains amine/imine groups that act as charge traps. Redistribution alters the trap density/distribution, affecting Poole—Frenkel emission and leakage current.
- direct or Fowler-Nordheim tunneling through thin polymer barriers, especially at high fields [8, 9].

So, the nonlinearity in Fig. 5 arises from the competition between Schottky emission and other mechanisms (Fowler–Nordheim tunneling and Poole–Frenkel emission) exacerbated by the composite's microstructure and PANI doping. The insulating polymer interlayers and defects further distort the ideal Schottky behavior. All of this is evident from Table I — as the barrier heights increase with ZnO content, the breakdown voltages decrease, which contradicts the classic Schottky behavior. This suggests that PANI doping disrupts the conduction mechanisms by introducing additional conduction paths to the composite.

4. Conclusions

In this study, we explored how ZnO-polymer composite varistors behave under electrical stress and how their performance changes with composition. It is found that adjusting the amount of ZnO directly influences key electrical properties adding more ZnO reduces the material's nonlinear response but allows it to handle higher voltages before breaking down. Notably, DC degradation induces profound, remarkable electrical changes while leaving the microstructure intact, as confirmed by comparative SEM analysis. These findings reveal that the dominant degradation mechanism is related to nanoscale PANI redistribution and interfacial barrier modification through Joule heating. The deviation from ideal Schottky emission in the $\ln(I) - \sqrt{V}$ characteristics emphasizes the complex interplay of conduction mechanisms, where Poole–Frenkel emission and tunneling compete with thermionic emission across the modified barriers. Although degradation in ceramic varistors reveals itself through phase changes at the grain boundaries, in the polymer-based system, it manifests itself through electrical aging behavior separated from microstructural evolution.

References

- [1] P.R. Bueno, J.A. Varela, E. Longo, *J. Eur. Ceram. Soc.* **28**, 505 (2008).
- [2] D. Xu, L. Shi, Z. Wu, Q. Zhong, X. Wu, J. Eur. Ceram. Soc. 29, 1789 (2009).
- [3] S. Bernik, S. Maček, A. Bui, J. Eur. Ceram. Soc. 24, 1195 (2004).
- [4] M. Peiteado, J. Fernández, A. Caballero, J. Eur. Ceram. Soc. 25, 2999 (2005).
- [5] C. Leach, Acta Mater. **53**, 237 (2005).
- [6] K. Eda, J. Appl. Phys. 49, 2964 (1978).
- [7] T.K. Gupta, J. Am. Ceram. Soc. 73, 1817 (1990).

- [8] G.D. Mahan, L.M. Levinson, H.R. Philipp, J. App. Phys. 50, 2799 (1979).
- [9] G. Mahan, L. Levinson, H. Philipp, Appl. Phys. Lett. 33, 830 (1978).
- [10] M. Peiteado, J.F. Fernández, A.C. Caballero, *J. Eur. Ceram. Soc.* 27, 3867 (2007).
- [11] M. Elfwing, R. Österlund, E. Olsson, *J. Am. Ceram. Soc.* **83**, 2311 (2000).
- [12] Y.W. Lao, S.T. Kuo, W.H. Tuan, *J. Electroceram.* **19**, 187 (2007).
- [13] S. Tkaczyk, *Physica E* **43**, 1179 (2011).
- [14] F.H. Cristovan, Synth. Met 161, 2041 (2011).
- [15] Q. Liu, X. Yao, X. Zhou, Z. Qin, Z. Liu, Scr. Mater. 66, 113 (2012).
- [16] H. Bidadi, S.M. Aref, M. Ghafouri, M. Parhizkar, A. Olad, J. Phys. Chem. Solids 74, 1169 (2013).
- [17] H. Bidadi, S.M. Aref, M. Ghafouri, M. Parhizkar, A. Olad, *Mater. Sci. Semi-cond. Process.* 16, 752 (2013).
- [18] H. Bidadi, A. Olad, M. Parhizkar, S.M. Aref, M. Ghafouri, *Vacuum* 87, 50 (2013).
- [19] H. Bidadi, S.M. Aref, M. Ghafouri, M. Parhizkar, A. Olad, *Cur. Appl. Phys.* 13, 355 (2013).
- [20] R. Parra, J. Rodriguez-Paez, J. Varela, M. Castro, *Ceram. Int.* 34, 563 (2008).
- [21] P. Kostić, O. Milosević, D. Uskoković, M. Ristić, $Physica\ B+C\ 150,\ 175,\ (1988).$
- [22] T.K. Gupta, W.G. Carlson, J. Mater. Sci. 20, 3487 (1985).
- [23] Y.M. Chiang, W. Kingery, L.M. Levinson, J. Appl. Phys. 53, 1765 (1982).
- [24] A. Iga, Jpn. J. Appl. Phys. 19, 201 (1980).
- [25] K. Sato, Y. Takada, T. Takemura, M. Ototake, J. Appl. Phys. 53, 8819 (1982).
- [26] K. Eda, A. Iga, M. Matsuoka, J. Appl. Phys. 51, 2678 (1980).
- [27] T.K. Gupta, W. Carlson, P. Hower, J. Appl. Phys. 52, 4104 (1981).
- [28] T. Corrales, F. Catalina, C. Peinado, N. Allen, E. Fontan, J. Photochem. Photobiol. A 147, 213 (2002).

- [29] J. Verdu, J. Rychly, L. Audouin, *Polym. Degrad. Stab.* 79, 503 (2003).
- [30] N.S. Allen, M. Edge, T. Corrales, A. Childs, C.M. Liauw, F. Catalina, C. Peinado, A. Minihan, D. Aldcroft, Polym. Degrad. Stab. 61, 183 (1998).
- [31] D.Y. Perera, *Prog. Org. Coat.* **50**, 247 (2004).
- [32] N.S. Allen, M. Edge, T. Corrales, F. Catalina, *Prog. Org. Cont.* 61, 139 (1998).
- [33] A.G. MacDiarmid, J.C. Chiang, A.F. Richter, *Synth. Met.* **18**, 285 (1987).
- [34] G.K. Elyashevich, L. Terlemezyan, I.S. Kuryndin, V.K. Lavrentyev, P. Mokreva, E.Y. Rosova, Y.N. Sazanov, Thermochim. Acta 374, 23 (2001).
- [35] A.H.I. Mourad, *Mater. Design* **31**, 918 (2010).
- [36] M. Ghafouria, M. Parhizkar, H. Bidadi, S.M. Aref, A. Olad, *Mater. Chem. Phys.* 147, 1117 (2014).
- [37] F. Tabrizi, M. Parhizkar, H. Bidadi, M. Ghafouri, Trans. Nonferrous Met. Soc. China 28, 1377 (2018).
- [38] H.C. Card, E.S. Yang, *IEEE Trans. Electron Devices* **24**, 397 (1977).
- [39] P. William, O.L. Krivanek, G. Thomas, J. Appl. Phys. 51, 3930 (1980).
- [40] S.A Pianaro, P.R Bueno, P. Olivi, E. Longo, J.A Varela, J. Mater. Sci. Mater. Electron. 9, 159 (1998).
- [41] M. Tu, W. Han, R. Zeng, S.M. Best, R.E. Cameron, *Colloids Surf. A* 407, 126 (2012).
- [42] L. Dai, Intelligent Macromolecules for Smart Devices: From Materials Synthesis to Device Applications, 1st ed., Springer-Verlag, London 2004.
- [43] Y.S. Lee, T.Y. Tseng, J. Am. Ceram. Soc. **75**, 1636 (1992).
- [44] D.R. Clarke, J. Am. Ceram. Soc. 82, 485 (1999).
- [45] L.M. Levinson, H.R. Philipp, Am. Ceram. Soc. Bull. 65, 639 (1986).